International Journal of Soft Computing 10 (6): 442-447, 2015
ISSN: 1816-9503

Image Compression Subband Method

Evgeniy G. Zhilyakov, Igor S. Konstantinov,
Andrey A. Chernomorets and Evgeniya V. Bolgova
Belgorod State National Research University, Pobedy Str., 85,
308015 Belgorod, Russia

Abstract: In this study, we present a image compression method based on the their subband decomposition on the eigenvectors of the subband matrix which achieves high compression ratios for a particular class of images. Some results of computing experiments are given.

Key words: Image, subarea of spatial frequencies, subband components, information subareas, decomposition on the eigenvectors of subband matrix

INTRODUCTION

The volume of the stored, transferred and processed digital images (Gonzalez and Woods, 2002; Petrou and Bosdogianni, 1999; Jain, 1989) constantly increases in modern information and telecommunication systems. In this regard development of new images compression methods allowing to raise extent of their compression without essential loss of visual quality is of interest (Miano, 1999; Sayood, 2012; Joshi *et al*., 2014; Thyagarajan, 2011). Data compression is important for quick transfer and storage efficiency of such content. Image processing requires intensive computation which can be burdened by equipment errors (Korsunov *et al*., 2014). Developments in many engineering and mathematics fields have been used in image compression. One of the main problems is highlighting and reducing the redundant information in an image. The methods to reduce bitmap representations in graphics files have been studied extensively (Sahnoun and Benabadji, 2015; Salomon, 2006; Salomon *et al*., 2010; Swamy *et al*., 2012) based on a number of lossy data coding formats (JPEG and JPEG 2000) (Pennebaker and Mitchell, 1993; Rabbani and Joshi, 2002).

Presently, an approach based on the so-called subband coding is becoming widespread (Caraiman, 2013; Gupta and Garg, 2012). In subband coding, an original image is replaced by a set of its components that reflect the frequency properties of the original image in various Spatial Frequency (SF) subdomains. The ability to realize image compression methods based on frequency representations is defined by the periodicity or quasiperiodicity of displayed processes in visual data.

Representations of the separate image $\Phi = \{f_{ik}\}$, i = 1, 2, ..., N, k = 1, 2, ..., M in the area of spatial frequencies >x, y as follows:

$$f_{ik} = \frac{1}{\pi^2}\int_{-\pi}^{\pi}\int_{-\pi}^{\pi} F(x, y)e^{jx(i-1)}e^{jy(k-1)}dxdy \quad (1)$$

Where:

f_{ik} = The brightness values of image Φ in the corresponding pixels with coordinates (i, j)
j = Imaginary unit ($j^2 = -1$)
F (x, y) = Frequency parameter as which it is most often used Fourier transformant F^{Φ} (x, y)

$$F^{\Phi}(x, y) = \sum_{k=1}^{M}\sum_{i=1}^{N} f_{ik}e^{-jx(i-1)}e^{-jy(k-1)}$$

are a mathematical basis for many image-processing tasks (Gonzalez and Woods, 2002; Jain, 1989; Hu *et al*., 2011). At the solution of practical tasks the Fourier transformant values usually are considered in the area of normalized frequencies u, v as follows:

$$-\pi \le u, v \le \pi \quad (2)$$

BACKGROUND

Formation of subband image components: Many image analysis and synthesis tasks can be solved using a partition of domain (Eq. 2) of the Fourier transform to a number of Subdomains of Spatial Frequencies (SSF) if Eq. 1 has the following form:

$$f_{ik} = \frac{1}{4\pi^2}\sum_{s=1}^{S}\sum_{r=1}^{R}\iint_{(u, v)\in V_{sr}} F^{\Phi}(u, v)e^{ju(i-1)}e^{jv(k-1)}dudv \quad (3)$$

Where:

$$V_{sr} = D_s \cap G_r \quad (4)$$

Corresponding Author: Evgeniy G. Zhilyakov, Belgorod State National Research University, Pobedy Str., 85, 308015 Belgorod, Russia

$$\begin{aligned} &D_s = [-u_{s2}, -u_{s1}) \cup [u_{s1}, u_{s2}) \\ &G_r = [-v_{r2}, -v_{r1}) \cup [v_{r1}, v_{r2}) \\ &s = 1, 2, ..., S \\ &r = 1, 2, ..., R \\ &u_{11} = 0, u_{S,2} = \pi, u_{s+1,1} = u_{s2} \\ &v_{11} = 0, v_{R,2} = \pi, v_{r+1,1} = v_{r2} \end{aligned} \quad (5)$$

In partition of frequency area (Eq. 2) to the subdomains V_{sr} (Eq. 4) the spatial frequency u takes values from the subband D_s of the x-axis of the SF plane and frequency v falls into subbands G_r of the y-axis.

Let's define that the subband component of an image Φ, corresponding to some SSF (Eq. 4) is image $Y_{sr} = \{y^{sr}_{ik}\}$, i = 1, ..., N, k = 1, ..., M which is defined by the separate item of Eq. 3:

$$y^{sr}_{ik} = \frac{1}{4\pi^2} \iint_{(x, y) \in V_{sr}} F^{\Phi}(u, v) e^{ju(i-1)} e^{jv(k-1)} du dv \quad (6)$$

In view of the fact that the subband component is completely defined by a two-dimensional segment of the Fourier transform corresponding to selected SSF than research of this component allows to judge properties of the initial image in the spatial area adequately. For example, the analysis of image subband component allows to reveal the image periodicity along a certain direction.

However, there is a problem in calculating the subband components because using definition (Eq. 6) is not possible. This requires the calculation of the integrals from the precomputed points in the continuum of the desired SF subdomain of two-dimensional segments of the Fourier transform. In this study, we proved the following statement.

Statement: The subband components $Y_{sr} = \{y^{sr}_{ik}\}$, i = 1, ..., N, k = 1, ..., M which elements are defined by condition (Eq. 6) can be calculated as follows:

$$Y_{sr} = A_s \Phi B_r \quad (7)$$

Where:

Φ = Matrix of the initial image

A_s and B_r = Subband matrixes $A_s = \{a^s_{in}\}$, i, n = 1, ..., N and $B_r = \{b^r_{km}\}$, k, m = 1, .., M, corresponding to SF subdomain V_{sr} and which elements values are calculated as follows

$$a^s_{in} = \frac{1}{2\pi} \int_{x \in D_s} e^{-jx(i-n)} dx, \; b^r_{km} = \frac{1}{2\pi} \int_{x \in G_r} e^{-jx(k-m)} dx \quad (8)$$

Recall that subbands D_s and G_r as defined in Eq. 5. It is easy to show that sum of the subband components (Eq. 7) under conditions (Eq. 4 and 5) is identical to the corresponding image:

$$\sum_{s=1}^{S} \sum_{r=1}^{R} Y_{sr} = \Phi$$

Note that operation (Eq. 7) matches the definition of filtering of individual subband components, e.g. when denoising images.

Image eigenvector decomposition of subband matrices: It can be demonstrated that A_s and B_r (Eq. 8) are symmetric and positively defined. Therefore, they have a complete system of orthonormal eigenvectors. For A_s-$\{\vec{q}^s_n\}$, n = 1, 2, ..., N and $\vec{q}^s_n = (q^s_{1n}, q^s_{2n}, ..., q^s_{Nn})^T$ and for B_r-$\{\vec{q}^s_m\}$, m = 1, 2, ..., M and $\vec{q}^s_m = (q^s_{1m}, q^s_{2m}, ..., q^s_{Mm})^T$. They correspond to the positive eigenvalues $\{\lambda^s_n\}$, n = 1, 2, ..., N, $\{\lambda^r_m\}$ and m = 1, 2, ..., M for which the following formulas are performed as follows:

$$\lambda^s_n \vec{q}^s_{ln} = A_s \vec{q}^s_n, \; n = 1, 2, ..., N \text{ and } \lambda^r_m \vec{q}^r_{lm} = B_r \vec{q}^r_{lm}, \; m = 1, 2, ..., M$$

$$\lambda^s_n \geq \lambda^s_{n+1} > 0, \; n = 1, 2, ..., N\text{-}1 \text{ and } \lambda^r_m \geq \lambda^r_{m+1} > 0, \; m = 1, 2, ..., M\text{-}1$$

Then, the subband matrices have the following eigenvector decomposition and values (Zhilyakov *et al*., 2007):

$$A_s = \sum_{n=1}^{N} \lambda^s_n \vec{q}^s_n (\vec{q}^s_n)^T = Q_s L_s Q_s^T$$

And:

$$B_r = \sum_{m=1}^{M} \lambda^r_m \vec{q}^r_m (\vec{q}^r_m)^T = Q_r L_r Q_r^T \quad (9)$$

Where:

Q_s and Q_r = Matrices whose columns are the eigenvectors of A_s and B_r

L_s and L_r = The diagonal matrices composed of the eigenvalues of A_s and B_r

$$Q_s = (\vec{q}^s_1, ..., \vec{q}^s_N), \; L_s = \text{diag}(\lambda^s_1, ..., \lambda^s_N)$$

And:

$$Q_r = (\vec{q}^r_1, ..., \vec{q}^r_m), \; L_r = \text{diag}(\lambda^r_1, ..., \lambda^r_M)$$

Thus, we obtain the following expression for the subband component definition by substituting correlation (Eq. 19) in expression (Eq. 7):

$$Y_{sr} = Q_s L_s Q_s^T \Phi Q_r L_r Q_r^T \quad (10)$$

The matrix of the form:

$$W_{sr} = Q_s^T \Phi Q_r \quad (11)$$

is considered as the eigenvector decomposition of image Φ of A_s and B_r. The following operation should be performed to restore the image subband component corresponding to the selected V_{sr}:

$$Y_{sr} = Q_s L_s W_{sr} L_r Q_r^T$$

Consequently, W_{sr} matrices completely save information about the subband components. However, they can have much smaller dimension because the eigenvalues of the subband matrices accurately Eq. 12:

$$\lambda^s_{J_s+i} \approx 0,\ i = 1, 2, ..., N\text{-}J_s$$

And:

$$\lambda^r_{J_r+k} \approx 0,\ k = 1, 2, ..., M\text{-}J_r \quad (12)$$

where, $J_s = 2[N.\Delta u_s/2\pi]+2$, $J_r = 2[M.\Delta u_r/2\pi]+2$, $\Delta u_s = u_{s2}\text{-}u_{s1}$ and $\Delta v_r = v_{r2}\text{-}v_r$. Here, [ ] is the integer part of a number. Property (Eq. 12) is established on the basis of the computational experiments on the subband matrix properties.

As specified in Eq. 12, the following representation is used as a sufficiently accurate approximation of the subband matrices:

$$\tilde{A}_s = Q_{1s} L_{1s} Q_{1s}^T \text{ and } \tilde{B}_r = Q_{1r} L_{1r} Q_{1r}^T \quad (13)$$

Where:

$$Q_{1s} = (\vec{q}^s_1, ..., \vec{q}^s_{J_s});\ L_{1s} = \text{diag}(\lambda^s_1, ..., \lambda^s_{J_s}) \text{ and}$$
$$Q_{1r} = (\vec{q}^r_1, ..., \vec{q}^r_{J_r});\ L_{1r} = \text{diag}(\lambda^r_1, ..., \lambda^r_{J_r})$$

Considering representation (Eq. 13), the following expression can be used to calculate the eigenvector decompositions of image Φ in V_{sr} approximately:

$$W_{1,sr} = Q_{1s}^T \Phi Q_{1r} \quad (14)$$

Then, the following transformation should be performed to recover the approximate value of the subband component that corresponds to the selected V_{sr}:

$$\tilde{Y}_{sr} = Q_{1s} L_{1s} W_{1,sr} L_{1r} Q_{1r}^T$$

Note that the number of W_{sr} elements obtained by each of the eigenvector decompositions of Φ, defined by Eq. 11, coincides with the number of image elements. For approximate calculation of Eq. 14, the dimension of the matrix $W_{1,sr}$ decreases significantly. The proposed image compression method is based on this fact.

In terms of the properties of the group of subband image components an approximate restoration of Φ^* of the original image can be performed based on an eigenvector decomposition set of $\{W_{1,sr}\}$ image for each V_{sr}, s = 1, 2, .., S and r = 1, 2, ..., R (the spatial frequency domain was divided on them) as follows:

$$\Phi^* = \sum_{s=1}^{S}\sum_{r=1}^{R} \tilde{Y}_{sr} = \sum_{s=1}^{S}\sum_{r=1}^{R} Q_{1s} L_{1s} W_{1,sr} L_{1r} Q_{1r}^T \quad (15)$$

Therefore, restoring the image information to store data on its eigenvector decomposition of subband matrices corresponding to each SF subdomain is sufficient.

Memory size required to store eigenvector decomposition results: There are several ways to reduce the memory size required to store the elements of $W_{1,sr}$, s = 1, 2, ..., S and r = 1, 2, ..., R.

Storing only the eigenvector decomposition matrices corresponding to the SF subdomains which contain the proportions of $P_{sr}(\Phi)$ (Zhilyakov *et al.*, 2014) of the energy of image Φ that exceed the specified threshold value T_1 (information SF subdomains):

$$P_{sr}(\Phi) > T_1 \quad (16)$$

Excluding the decomposition matrix of certain elements from the stored memory substantially reduces its bit representations. These elements correspond to the non-information SF subdomains that have image proportion energy $P_{sr}(\Phi) \leq T_1$.

Level-quantization of the element values of $W_{1,sr}$. This provides a significant reduction of the bit representations required to store matrix data.

Reversible compression of the results of the above operations by applying known or original compression algorithms such as Huffman codes.

The previous operations constitute an image compression method based on the decomposition of the subband components on the eigenvectors of the corresponding subband matrices.

Computational experiments: To test the efficiency of the proposed method, the standard deviation of the restored image after compression of image Φ^* (Eq. 15) was calculated relative to the original image Φ which is as follows:

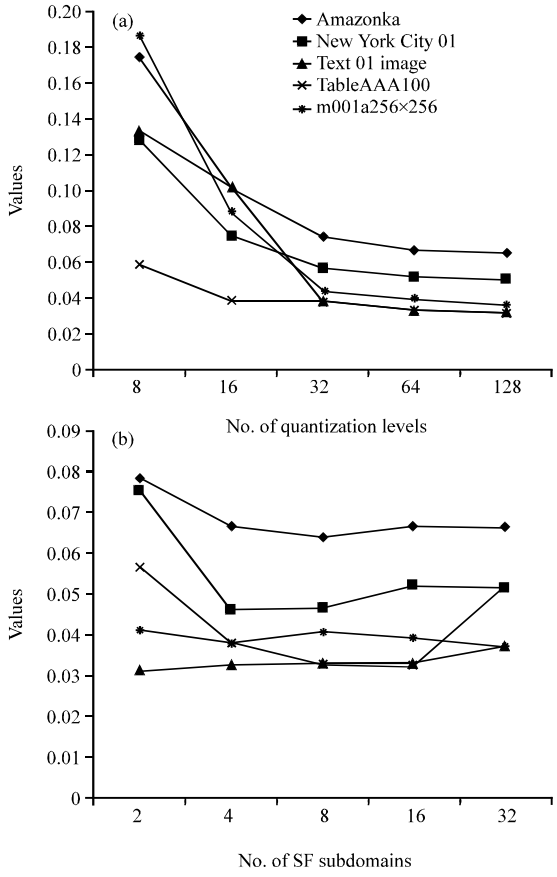

Fig. 1: Standard deviation of the restored image relative to the initial image: a) versus the number of quantization levels and b) versus the number of SF subdomains

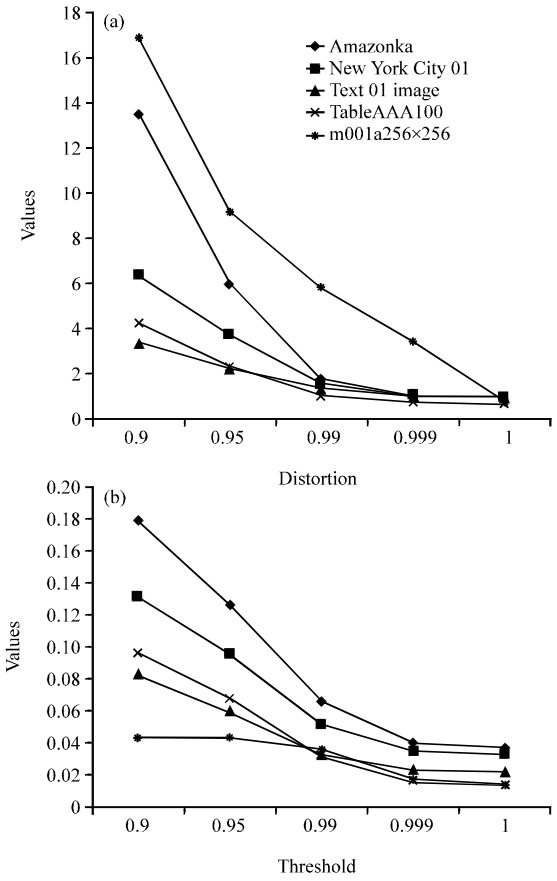

Fig. 2: a) Compression ratio and b) distortion of the restored image versus values of the threshold proportion energy m

$$\delta = \frac{\left\|\Phi-\Phi^{*}\right\|}{\left\|\Phi\right\|} \qquad (17)$$

The compression ratio was also calculated as the ratio of the bit number of the original image to that of the compressed image. Experiments were conducted to convert the images of various types (they are placed in site https://yadi.sk/d/56HTaegjj9TGa) at different quantization level and SF subdomain values. The calculation results are given in Fig. 1 and 2.

The noise value (Eq. 17) of the restored image at various quantization levels is proportional to the level number and practically does not depend on the number of SF subdomains (Fig. 1).

In the experiment, we selected such values of T_1 (Eq. 16) that when compressing Φ there were used decompositions $W_{1, sr}$ (Eq. 14) of image Φ in that spatial frequency subdomains V_{sr} which total energy correspond to 99% of the total energy of the test image Φ.

Figure 2 shows the above coefficient and values (Eq. 23) of the restored image against those of the threshold proportion m of the image energy at 64 quantization levels and 16 SF subdomains (m is used to identify a set of data subdomains as the minimal set which corresponds to m% of the total energy of the test image). Figure 2 shows that the compression ratio decreases significantly with increasing m and noise is reduced.

For the purpose of visual comparison of results of application of a subband compression method and the most known compression methods JPEG and JPEG2000 the increased fragments of tested image splash (it is placed in the internet to the address stated above) and the results of its compression with rather big coefficient of compression 50 are given in Fig. 3. Thus, the mean square deviation (Eq. 17) and PSNR (peak signal-to-noise ratio) of compression results was calculated.

Visual comparison of the restored images presented in Fig. 3 shows that at great values of coefficient of separate images compression the results of the offered

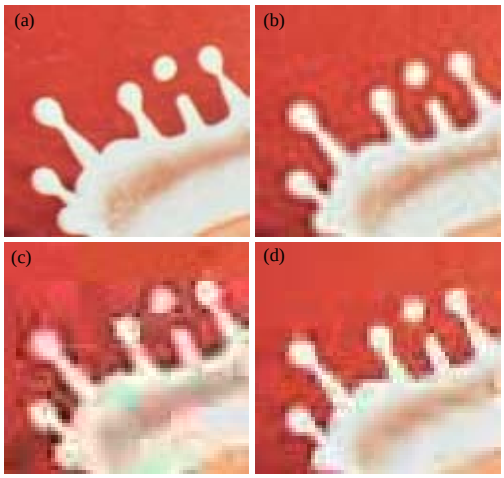

Fig. 3: Increased fragments of tested image and the results of its compression using different methods (coefficient of compression is equal to 50): a) tested image; b) subband mehod (δ = 0.020; PSNR δ = 36.5); c) JPEG (δ = 0.067; PSNR = 26.1) and d) JPEG2000 (δ = 0.036; PSNR = 31.4)

compression method application (Fig. 3b) have the best visual quality, for example, less distorted the image objects borders, than at algorithms JPEG and JPEG2000 application.

CONCLUSION

This study has shown high quality restoration and compression of images using a compression method based on the eigenvector decomposition of subband matrices. The proposed method demonstrates higher quality compression and restoration than the JPEG and JPEG2000 algorithms. The compression method that employs the decomposition of the quasicyclic subband components of an image was designed to compress images with a higher degree of compression and restore them with less distortion compared with the aforementioned algorithms.

ACKNOWLEDGEMENT

The study has been conducted under subsidy #14.581.21.0003 (project ID-RFMEFI58114X0003) with the Ministry of Education and Science of the Russian Federation.

REFERENCES

Caraiman, S., 2013. Quantum image filtering in the frequency domain. Adv. Electr. Comput. Eng., 13: 77-84.

Gonzalez, R.C. and R.E. Woods, 2002. Digital Image Processing. 2nd Edn., Prentice Hall, New Jersey, pp: 793.

Gupta, M. and A.K. Garg, 2012. Analysis of image compression algorithm using DCT. Int. J. Eng. Res. Appl., 2: 515-521.

Hu, J., J. Deng and J. Wu, 2011. Image compression based on improved FFT algorithm. J. Networks, 6: 1041-1048.

Jain, A.K., 1989. Fundamentals of Digital Image Processing. Prentice Hall, Englewood Cliffs, NJ., ISBN-10: 0133361659, Pages: 569.

Joshi, M.A., M.S. Raval, Y.H. Dandawate, K.R. Joshi and S.P. Metkar, 2014. Image and Video Compression: Fundamentals, Techniques and Applications. Chapman and Hall/CRC, UK., Pages: 236.

Korsunov, N.I., I.S. Konstantinov and A.A. Nachetov, 2014. Error correction method results in a multiplication of the supercomputer. Res. J. Appl. Sci., 9: 1120-1123.

Miano, J., 1999. Compressed Image File Formats: JPEG, PNG, GIF, XBM, BMP. Addison-Wesley Professional, USA., Pages: 288.

Pennebaker, W.B. and J.L. Mitchell, 1993. JPEG: Still Image Data Compression Standard. Springer, New York, USA., ISBN-13: 9780442012724, Pages: 638.

Petrou, M. and P. Bosdogianni, 1999. Image Processing: The Fundamentals. John Wiley and Sons Inc., New Jersey.

Rabbani, M. and R. Joshi, 2002. An overview of the JPEG 2000 still image compression standard. Signal Process. Image Commun., 17: 3-48.

Sahnoun, K. and N. Benabadji, 2015. Satellite image compression technique using noise bit removal and discrete wavelet transform. Int. J. Imaging Rob., 15: 57-64.

Salomon, D., 2006. The Compression of Data, Images and Sound. Tehnosfera, Moscow, Russia, Pages: 368.

Salomon, D., G. Motta and D. Bryant, 2010. Handbook of Data Compression. Springer, Berlin, Germany, Pages: 1361.

Sayood, K., 2012. Introduction to Data Compression. 4th Edn., Morgan Kaufmann Publishers, San Francisco, USA., Pages: 768.

Swamy, S., A.S. Mamatha and V. Singh, 2012. Low-complexity and high-quality image compression algorithm for onboard satellite. Int. J. Comput. Appl., 47: 24-31.

Thyagarajan, K.S., 2011. Still Image and Video Compression with MATLAB. John Wiley and Sons, New York, USA., ISBN-13: 9781118097762, Pages: 428.

Zhilyakov, E.G., A.A. Chernomorets and E.V. Bolgova, 2014. About image decomposition on the eigenvectors of subband matrix. Belgorod State Univ. Sci. Bull. Hist. Political Sci. Econ. Inf. Technol. Ser., 15: 185-189.

Zhilyakov, E.G., A.A. Chernomorets and I.V. Lysenko, 2007. Method of determination of images energy shares exact values in the given frequency intervals. Prob. Radioelectronics Radiolocating Facil. Ser., 4: 115-123.